Toward Accessible Surgical Robotics Research: Wrist-Mapped Teleoperation of a 7-DoF Industrial Manipulator

Lou Genoud[1] Richard Clough[2,3] Etienne Burdet[2] Joshua Brown[1]

***Abstract*— Industrial robotic arms could broaden access to surgical robotics research, but whole-arm inverse kinematics can distribute orientation commands across redundant joints, producing undesirable proximal motion in confined multi-robot workspaces. This work compares two wrist-orientation strategies for teleoperation of a seven degrees-of-freedom (DoF) KUKA LBR iiwa 7 R800 using an Omega.7 haptic interface. Both modes use Cartesian differential inverse kinematics for translation. Mode 1 resolves orientation hierarchically within the approximate translational null space, whereas Mode 2 maps master pitch and roll directly to joints J6 and J7. Identical time-stamped master inputs were replayed from the same initial robot configuration. Mode 2 strongly reduced cross-axis and proximal joint motion during isolated rotations and substantially reduced J4 excursion during coupled translation–rotation, at the cost of increased translational tracking error. Hybrid direct mapping therefore provides predictable joint allocation, but sacrifices independent yaw control and automatic redistribution near joint limits. Future work will evaluate Cartesian accuracy, collision clearance, and independent yaw control and apply the system to study surgeon performance in complex teleoperation tasks.**

I. Introduction

Commercial teleoperated robotic surgical systems provide tremor reduction, motion scaling, and distal instrument dexterity. Systems including the da Vinci Surgical System, Versius Surgical System, and Symani Surgical System incorporate wristed instruments for fine manipulation [1], [2], [3]. However, their lack of control flexibility, as well as their high acquisition and maintenance costs, limit their accessibility for research. Adapting six or seven-DoF industrial arms already available in robotics laboratories without extensive setup development could broaden participation in surgical robotics research.

Open-source frameworks such as LBR-Stack support real-time control of KUKA LBR robots [4]. Seven-DoF arms have also been investigated for redundancy-based obstacle avoidance and foot-controlled laparoscopic assistance [5], [6]. These studies primarily address laparoscopic procedures, where remote-centre-of-motion constraints maintain instrument alignment with a trocar [7]. Open microsurgery instead requires local wrist-like tool manipulation without a fixed trocar pivot. One example is open anastomosis, in which structures such as blood vessels are joined using wrist-driven instrument movements requiring high dexterity.

[1]Department of Surgery & Cancer, and [2]Department of Bioengineering, Imperial College of Science, Technology and Medicine, London UK.
[3]Royal Marsden Hospital, London UK.
The authors thank Dr Fabio Tatti of Imperial College's Hamlyn Centre for Robotic Surgery for technical assistance in the setup of the robots.

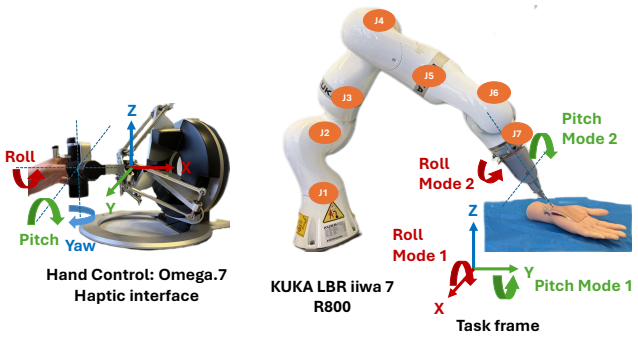

Fig. 1: Teleoperation setup and reference frames. Mode 1 resolves orientation about the Cartesian task-frame axes at the gripper, whereas Mode 2 maps the Omega.7 pitch and roll directly to J6 and J7.

This work investigates teleoperation of the KUKA LBR iiwa 7 R800 for wrist-like tool manipulation in open microsurgery. It compares translation-priority Cartesian orientation control with hybrid direct joint mapping, in which the Omega.7 pitch and roll inputs control J6 and J7, respectively. The modes are evaluated using identical recorded master inputs to quantify their angular response, joint allocation, and gripper-tip motion. The results demonstrate that direct mapping provides predictable distal joint allocation with negligible proximal joint displacement during the tested isolated pitch and roll sequences.

II. Motion Allocation in Cartesian IK

The KUKA LBR iiwa 7 R800 is a seven-axis serial manipulator with a two-axis wrist comprising J6 and J7 [8]. The technical challenge of using industrial robotic arms to simulate surgical robots is to coordinate translational and angular teleoperation while controlling how orientation commands are allocated across the redundant robot joints.

Conventional, whole-arm IK solvers typically allow all seven joints to contribute to the solution unless joint constraints, weighting, or redundancy objectives are specified. Consequently, angular commands may produce motion in both the proximal and distal joints, increasing the robot's swept volume. In a confined workspace shared by multiple robots, this behaviour can increase the risk of robot to robot collisions and demand challenging collision avoidance constraints on the IK solver.

Achieving precise angular control while preserving linear tracking requires explicit consideration of how motion is allocated across the robot joints. Cartesian differential IK

provides general tool-pose control and can incorporate task priorities, joint weighting, and joint-limit avoidance [9]. However, solving translation and orientation independently can introduce cross-task motion. Translation-only IK may generate unintended angular velocity, while angular-only IK may generate linear motion unless the linear velocity or rotation pivot is explicitly constrained. Damping and active constraints can improve robustness but may reduce Cartesian tracking accuracy near singularities or joint limits [9], [10]. Furthermore, because redundant manipulators admit multiple joint solutions for the same Cartesian motion, the resulting joint trajectory depends on the initial configuration and redundancy-resolution strategy. Consequently, a repeated Cartesian trajectory may not produce a repeated joint trajectory [11].

The LBR iiwa R800 is teleoperated using an Omega.7 haptic device (Force Dimension), which provides six-DoF (three translational and three rotational) and one gripper DoF. Its translational workspace measures $160\ \mathrm{mm}$ in diameter and $110\ \mathrm{mm}$ in depth, while its rotational workspace is $240^\circ \times 140^\circ \times 180^\circ$ [12].

The Omega.7 served only as a position and orientation input device, with no force feedback rendered through the handle or actuated gripper in either mode. Visual feedback was provided by direct observation of the robot and tool. Haptic rendering under the hybrid joint mapping remains future work.

III. Comparison between Cartesian orientation control and hybrid direct joint mapping

Both strategies prioritise Cartesian translation and differ in how wrist orientation is introduced. Both modes use the same clutching mechanism, allowing the operator to reposition the Omega.7 without commanding robot motion.

For Cartesian control (Mode 1), the desired angular motion is resolved using a translation-priority hierarchical damped least-squares differential IK solver. In Mode 2, selected master inputs are assigned to specific robot joints, with the Omega.7 pitch and roll mapped directly to distal joints J6 and J7, respectively.

For a task Jacobian $\mathbf{J}_x$, the damped pseudoinverse is defined as

$$\mathbf{J}_x^{\#} = \mathbf{J}_x^T \left(\mathbf{J}_x \mathbf{J}_x^T + \lambda^2 \mathbf{I}\right)^{-1}, \tag{1}$$

where λ is the damping coefficient.

In Mode 1, the relative motion of the Omega.7 is converted into a desired linear velocity $\mathbf{v}_c$ and angular velocity $\boldsymbol{\omega}_c$. Translation is solved as the primary task:

$$\dot{\mathbf{q}}_v = \mathbf{J}_v^{\#} \mathbf{v}_c, \qquad \mathbf{N}_v = \mathbf{I} - \mathbf{J}_v^{\#} \mathbf{J}_v. \tag{2}$$

Orientation is then resolved within the approximate translational null space:

$$\dot{\mathbf{q}}_{M1} = \dot{\mathbf{q}}_v + \mathbf{N}_v \left(\mathbf{J}_\omega \mathbf{N}_v\right)^{\#} \left(\boldsymbol{\omega}_c - \mathbf{J}_\omega \dot{\mathbf{q}}_v\right), \tag{3}$$

where $\mathbf{J}_v$ and $\mathbf{J}_\omega$ are the linear and angular components of the robot Jacobian. This hierarchy prioritises Cartesian translation while allowing all seven joints to contribute to the orientation solution. The Jacobian is evaluated at a configurable pivot located at the centre of the gripper jaws, corresponding to the user's grasp point on the Omega.7 handle.

Hybrid joint mapping (Mode 2) combines Cartesian translation with direct distal joint control. The clutch-relative pitch and roll of the Omega.7 define targets for J6 and J7:

$$q_6^* = q_{6,0} + k_6 \Delta\theta_\Omega, \qquad q_7^* = q_{7,0} + k_7 \Delta\phi_\Omega, \tag{4}$$

where $q_{6,0}$ and $q_{7,0}$ are the robot joint positions at clutch engagement and k_6 and k_7 are the mapping gains. A bounded proportional controller converts the resulting joint errors into direct velocities $\dot{q}_{6,d}$ and $\dot{q}_{7,d}$. These are added to the Cartesian translational IK solution:

$$\dot{\mathbf{q}}_{M2} = \beta \left(\dot{\mathbf{q}}_v + \mathbf{e}_6 \dot{q}_{6,d} + \mathbf{e}_7 \dot{q}_{7,d}\right), \tag{5}$$

where $\mathbf{e}_6$ and $\mathbf{e}_7$ select J6 and J7, and $\beta \leq 1$ applies coordinated velocity limiting. Translational IK retains all seven joints, while the unprojected direct wrist commands produce the geometry-dependent TCP motion quantified below.

Both controllers operated at $200\ \mathrm{Hz}$. Mode 1 used adaptive damping, with $\lambda_{\max} = 0.05$ and damping activated for $\sigma_{\min} < 0.10$, together with a Cartesian angular-velocity limit of $1.20\ \mathrm{rad\,s^{-1}}$. For Mode 2, $k_6 = k_7 = 1.0$, the joint-position servo gain was $K_p = 7.0\ \mathrm{s^{-1}}$, and J6/J7 target displacements were limited to $\pm 70^\circ$ and $\pm 120^\circ$, respectively. Joint velocities were limited to $4.0\ \mathrm{rad\,s^{-1}}$; when required, the complete velocity vector was uniformly scaled by a runtime factor $\beta = \min(1, \min_i \dot{q}_{i,\max}/|\dot{q}_i^*|)$.

IV. Evaluation

The two control modes were evaluated using the same time-stamped Omega.7 recording captured upstream of all mode-specific transformations. The raw master pose and clutch state were replayed from the same initial robot configuration, $q_0 = [10, 45, 20, -80, -10, 0, 45]^\circ$, ensuring that differences in robot motion resulted from the control strategy rather than variations in operator input. Translation was disabled during these isolated angular trials; they therefore characterise angular allocation and cross-axis leakage rather than coupled translation–rotation performance. Pitch and roll were evaluated separately. Angular leakage was evaluated in Cartesian space from the gripper orientation obtained through forward kinematics. The orientation change was expressed as a rotation vector in the fixed robot task frame, and leakage was defined as the magnitude of its components orthogonal to the commanded pitch or roll axis. To account for differences in achieved primary-axis amplitude between controllers, leakage was normalised by the achieved on-axis response of each trial, $L = \max_t \|\boldsymbol{\theta}_\perp(t)\|_2 / \max_t |\theta_\parallel(t)|$, using a trial-level denominator to avoid singular ratios near zero crossings.

Gripper-tip motion was quantified from forward kinematics. For Mode 2, the J6-to-tip offset was $434\ \mathrm{mm}$, comprising $154\ \mathrm{mm}$ from J6 to the flange and $280\ \mathrm{mm}$ from the flange to the prototype gripper tip. The expected displacement under J6 rotation is $d = 2 r_6 \sin(|\theta|/2)$; at the configured

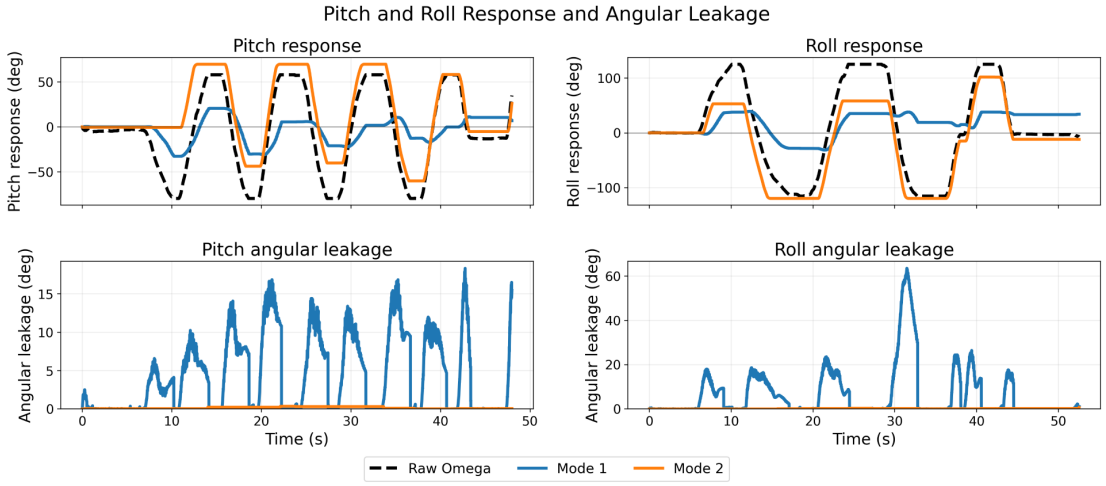

Fig. 2: Pitch and roll responses to identical recorded Omega.7 commands. The upper row compares the raw master input with the angular response produced by each control mode. The lower row shows the corresponding off-axis angular leakage.

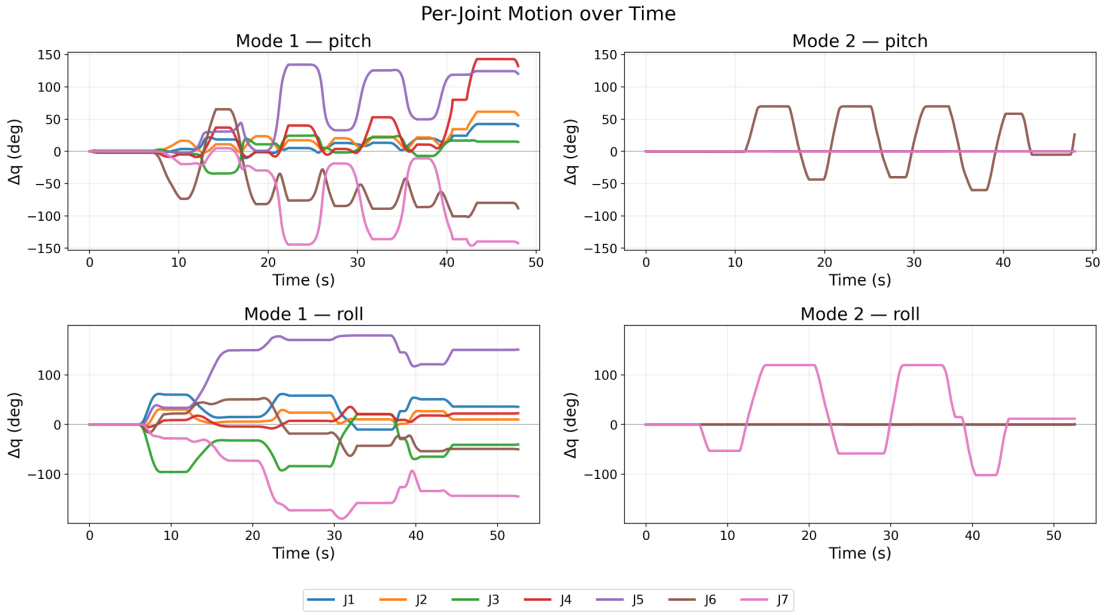

Fig. 3: Joint displacement relative to the initial robot configuration during isolated pitch and roll commands.

70° pitch limit this predicts 498 mm, compared with a measured maximum excursion of 496 mm. By contrast, J7 was approximately aligned with the tool axis and produced only 5.05 mm maximum tip excursion during roll.

Figure 2 compares the angular response produced by the two modes. Mode 2 followed the direction and switching sequence of the master pitch and roll inputs through its predetermined J6 and J7 mappings, with the response amplitude limited by the configured gains and saturation bounds. Mode 1 produced a distributed and nonlinear response in the tested configuration because the Cartesian orientation command was distributed across the redundant kinematic chain. After normalisation by the achieved primary response, peak cross-axis leakage was 56.1% and 160.9% for Mode 1 during pitch and roll, respectively, compared with 0.505% and 0.557% for Mode 2. The roll value indicates that in this tested Mode 1 configuration, the peak off-axis response exceeded the achieved primary-axis rotation.

The corresponding joint trajectories are shown in Fig. 3. Mode 1 distributed both pitch and roll motion across multiple proximal and distal joints. In contrast, during the isolated angular trials, Mode 2 confined the commanded angular motion to J6 or J7 while the remaining joints exhibited negligible displacement. These results demonstrate the predetermined joint allocation provided by direct mapping and demonstrated negligible proximal joint displacement during the isolated angular commands. Because J4 governs the principal elbow motion, its mean absolute displacement from the initial angle was used as a proxy for collision-relevant proximal-arm excursion. In Mode 1, this displacement was 31° during pitch and 11° during roll, whereas J4 remained stationary in Mode 2 (Fig. 3).

To assess whether this behaviour persisted when translation and rotation were commanded simultaneously, a repre-

TABLE I: Performance during the representative coupled translation–rotation sequence.

Metric	Mode 1	Mode 2
Translation RMSE [mm]	43.0	57.3
Peak translation error [mm]	163.2	254.6
Mean $\lvert\Delta q_4\rvert$ [deg]	76.3	4.84
Peak $\lvert\Delta q_4\rvert$ [deg]	164.8	16.0
Minimum β	1.00	1.00

sentative coupled sequence containing translation, pitch, and roll was replayed through both controllers. This sequence was intended as a controller-level coupled-motion test rather than a microsurgical-scale trajectory.

Mode 1 achieved lower translational tracking error, whereas Mode 2 substantially reduced proximal J4 motion. Coordinated velocity limiting did not activate in either mode ($\beta_{\min} = 1$), indicating that velocity saturation did not account for the difference in translational tracking. During Mode 2, peak J6 and J7 displacements were $48.0°$ and $10.3°$, respectively. The suitability of each control mode therefore depends strongly on the surgical task, particularly its requirements for Cartesian accuracy, wrist-centered manipulation, and motion scaling. These excursions characterise the present full-size industrial robot, long prototype gripper, and full-range controller-characterisation sweep rather than a representative microsurgical trajectory. Task experiments therefore use an enlarged phantom and a restricted angular range; translation to millimetre-scale surgical manipulation would require mechanical scaling, a distal rotation axis closer to the tool tip, or active pivot compensation.

V. Discussion and Future Work

This work compared Cartesian orientation control with hybrid direct joint mapping for teleoperation of a seven-DoF industrial robot. In the tested configuration, direct mapping reproduced the intended wrist-like motion by assigning master pitch and roll to J6 and J7, respectively, while limiting proximal joint motion. This approach provides predictable and repeatable joint-space behaviour, but does not inherently guarantee greater Cartesian precision because distal joint rotations can induce tool-tip translation. The comparatively large Mode 1 leakage and joint excursions are specific to the evaluated initial configuration and controller parameterisation and may depend on projected-Jacobian conditioning, damping, and task feasibility; they should therefore not be interpreted as an inherent limitation of whole-arm Cartesian IK.

The main limitations of the work are the absence of independent yaw control and the need to tune angular motion scaling. Reduced proximal motion may improve collision clearance in confined multi-robot workspaces, but joint excursion alone does not establish minimum separation between robot links. Likewise, predictable distal joint allocation does not guarantee Cartesian accuracy, since direct wrist rotations induce tool-tip translation. Future work will therefore evaluate task-scale Cartesian accuracy and collision clearance across a wider range of initial configurations and coupled trajectories. The integration of an additional rotational DoF at the gripper will also be explored to enable independent yaw control. Additionally, while the comparison of control metrics is complete, ethical approval for a full evaluation study with expert surgeons is in progress, limiting qualitative feedback to that of a single expert, who is also a co-author.

During formative testing, a microsurgeon co-author with experience using the Symani Surgical System reported smoother tool motion and greater range of motion with hybrid mapping. This preliminary observation motivates the hypothesis that direct wrist-to-joint correspondence may improve perceived intuitiveness; intuitiveness was not measured in the present evaluation. A surgeon study will test this hypothesis using task-performance measures and established workload and usability questionnaires.

DISCLOSURE OF INTERESTS

The authors have no competing interests to declare.

References

[1] A. L. G. Morrell, A. C. Morrell-Junior, A. G. Morrell, J. M. F. Mendes, F. Tustumi, L. G. De-Oliveira-E-Silva, and A. Morrell, "The history of robotic surgery and its evolution: when illusion becomes reality," *Revista do Colégio Brasileiro de Cirurgiões*, vol. 48, p. e20202798, 2021.

[2] J. Morton, R. H. Hardwick, H. S. Tilney, A. M. Gudgeon, A. Jah, L. Stevens, S. Marecik, and M. Slack, "Preclinical evaluation of the versius surgical system, a new robot-assisted surgical device for use in minimal access general and colorectal procedures," *Surgical endoscopy*, vol. 35, no. 5, pp. 2169–2177, 2021.

[3] A. Savastano and S. Rizzo, "A novel microsurgical robot: preliminary feasibility test in ophthalmic field," *Translational Vision Science & Technology*, vol. 11, no. 8, pp. 13–13, 2022.

[4] M. Huber, C. E. Mower, S. Ourselin, T. Vercauteren, and C. Bergeles, "Lbr-stack: Ros 2 and python integration of kuka fri for med and iiwa robots," *arXiv preprint arXiv:2311.12709*, 2023.

[5] M. Karnam, M. Zelechowski, P. C. Cattin, G. Rauter, and N. Gerig, "User-specified inverse kinematics taught in virtual reality reduce time and effort to hand-guide redundant surgical robots," *Communications engineering*, vol. 4, no. 1, p. 20, 2025.

[6] S. Gholami, L. Munier, M. Bouri, and A. Billard, "Four-handed solo laparoscopic anastomosis with the support of supernumerary robotic arms," in *2025 47th Annual International Conference of the IEEE Engineering in Medicine and Biology Society (EMBC)*. IEEE, 2025, pp. 1–7.

[7] J. Sandoval, H. Su, P. Vieyres, G. Poisson, G. Ferrigno, and E. De Momi, "Collaborative framework for robot-assisted minimally invasive surgery using a 7-dof anthropomorphic robot," *Robotics and Autonomous Systems*, vol. 106, pp. 95–106, 2018.

[8] *LBR iiwa: LBR iiwa 7 R800, LBR iiwa 14 R820—Specification*, Version v5 ed., KUKA Roboter GmbH, Augsburg, Germany, Jan. 2015. [Online]. Available: https://www.ingegneria.unicampania.it/images/laboratori/2025/aggiornamento_e_schede/Spez_LBR_iiwa_en.pdf

[9] D. Schinstock, T. Faddis, and R. Greenway, "Robust inverse kinematics using damped least squares with dynamic weighting," in *NASA. Johnson Space Center, Conference on Intelligent Robotics in Field, Factory, Service and Space (CIRFFSS 1994), Volume 2*, no. AIAA PAPER 94-1299-CP, 1994.

[10] L. Zhang, H. Du, Z. Qin, Y. Zhao, and G. Yang, "Real-time optimized inverse kinematics of redundant robots under inequality constraints," *Scientific Reports*, vol. 14, no. 1, p. 29754, 2024.

[11] M. Safeea, R. Bearee, and P. Neto, "A modified dls scheme with controlled cyclic solution for inverse kinematics in redundant robots," *IEEE Transactions on Industrial Informatics*, vol. 17, no. 12, pp. 8014–8023, 2021.

[12] Force Dimension, *omega.7 Haptic Device: Force Feedback Interface*, Nyon, Switzerland, product specification sheet. [Online]. Available: https://www.forcedimension.com/images/doc/specsheet_-_omega7.pdf